Intermodulation in Capacitively Coupled Microelectromechanical Filters

Ari T. Alastalo and Ville Kaajakari, *Member, IEEE*

***Abstract*—A compact model for third-order intermodulation in capacitively coupled microelectromechanical filters is derived. A simple expression for the input third-order intercept point is given. This is valuable in designing micromechanical filters, for example, for communication applications. The validity of the analytic model is verified with numerical harmonic-balance simulations and experimental measurements.**

***Index Terms*—Communication systems, filter distortion, filters, intermodulation distortion, microelectromechanical devices.**

I. Introduction

WIRELESS communication devices rely on high-quality-factor ceramic, SAW, or FBAR filters for RF and IF filtering. While these macroscopic filters offer excellent performance, the cost and size make them unattractive for portable devices. Consequently, receiver architectures such as direct conversion have been developed in order to reduce the need for off-chip components [1]. However, it is unlikely that the high-Q filters can completely be eliminated.

Micromechanical resonators are a potential replacement for off-chip filters due to their compact size and integrability with IC electronics [2]. The demonstrated quality factors of microresonators, $Q > 100\,000$ at 10 MHz [3] and $Q > 1\,000$ at 1 GHz [4], are comparable to their macroscopic counterparts. Unfortunately, as the resonator size is reduced, its power handling capacity and linearity are also lowered [5]. In filter applications, signal intermodulation (IM) due to odd-order nonlinearities is especially detrimental as it can result in unwanted frequency components within the filter passband. For example, cubic mixing of two fundamental signals having frequencies ω_1 and ω_2 results in third-order intermodulation (IM3) products at frequencies $2\omega_1 - \omega_2$ and $2\omega_2 - \omega_1$. Consequently, a useful measure of filter linearity is the third-order intercept point (IP3) defined as the crossing point of the linear extrapolations of the small-signal fundamental current (or voltage or power) and the IM3 current (or voltage or power) in the filter output. The signal level at the filter input, corresponding to IP3, is termed IIP3.

In this letter, the first published closed-form expression for in-band IIP3 is given for capacitively coupled microresonators, and the result is verified with simulations and experiments. The analysis differs from prior modeling where off-resonance forces were considered [6]. Here, the filter passband output currents are considered directly and all nonlinear terms are included to third-order. The results in this letter provide a practical starting point in evaluating and designing the microresonators for commercial filter applications.

Manuscript received January 4, 2005; revised February 22, 2005. This work was supported by the Academy of Finland under Grant 20542 and by Aplac Solutions. The review of this letter was arranged by Editor J. Sin.

The authors are with Microsensing, VTT Information Technology, VTT Technical Research Center of Finland, FIN-02044 VTT Espoo, Finland (e-mail: ari.alastalo@vtt.fi, ville.kaajakari@vtt.fi).

Digital Object Identifier 10.1109/LED.2005.846589

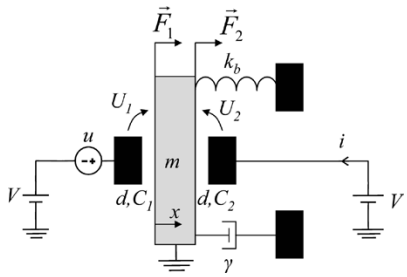

Fig. 1. Harmonic resonator (k_b, m, and γ) coupled capacitively for filtering of an electronic signal u. Signal u near the resonance excites mechanical motion that is sensed as current i.

II. Analysis

Fig. 1 shows a simplified model for a capacitively coupled mechanical resonator used as a filter. Here V is the bias voltage, u is the small-signal input voltage, and i is the current at the filter output. The zero-voltage gap of the input and output transducers is denoted by d and x is the displacement of the resonating mass m. The spring constant and the damping coefficient of the resonator are k_b and γ, respectively. The resonator quality factor is given by $Q = \sqrt{k_b m}/\gamma$. The capacitance values of the input and output transducers are $C_1 = \epsilon_0 A/(d+x)$ and $C_2 = \epsilon_0 A/(d-x)$, where A is the area of the transducer electrodes. The voltages across the transducers are $U_1 = V + u$ and $U_2 = V$, and the forces exerted by the transducers to the resonating mass are $F_i = (1/2)U_i^2 \partial C_i/\partial x$, $i \in \{1, 2\}$.

For small gaps, capacitive nonlinearities dominate and mechanical spring nonlinearities do not contribute to IIP3 [5]. Thus, the equation of motion for the resonator in Fig. 1, taking capacitive nonlinearities into account up to third order in small parameters $\bar{u} \equiv u/V$ and $\xi \equiv x/d$, is

$$m\ddot{\xi} + \gamma\dot{\xi} + \bar{k}\xi = -k_e\bar{u} + k_e\left[2\bar{u}\xi - \frac{\bar{u}^2}{2} + 4\xi^3 - 3\bar{u}\xi^2 + \bar{u}^2\xi\right]. \tag{1}$$

where $k_e \equiv \eta V/d$, with $\eta \equiv C_0 V/d$ and $C_0 \equiv \epsilon_0 A/d$, is the electromechanical spring constant and $\bar{k} \equiv k_b - 2k_e$. The time derivative is denoted with a dot. The output current $i = d(C_2 U_2)/dt$ can be expanded as

$$\bar{i} \equiv \frac{i}{d} = \eta\left(1 + 2\xi + 3\xi^2 + 4\xi^3 + \cdots\right)\dot{\xi}. \tag{2}$$

We use a high-Q approximation such that motion ξ has no frequency components outside the resonator passband. Thus, for signals near the resonance, only the linear force term and the three third-order force terms in (1) contribute to the motion. Similarly, only the first and third terms in (2) contribute to the in-band current.

A two-tone IM3 test is made with a signal $\bar{u}(t) = \bar{u}_0(\cos\omega_1 t + \cos\omega_2 t)$ where ω_1 and ω_2 are inside the filter passband. The resulting linear solution to (1), $\xi_{\rm lin} = -q\bar{u}_0\,(\sin\omega_1 t + \sin\omega_2 t)$, and (2) give the linear fundamental current

$$\bar{i}_{\rm fund} = \eta\dot{\xi}_{\rm lin} = -\eta q\bar{u}_0(\omega_1\cos\omega_1 t + \omega_2\cos\omega_2 t) \qquad (3)$$

where $q \equiv k_e Q/\bar{k}$. The main nonlinear contributions to the current (2) at $\omega_3 = 2\omega_1 - \omega_2$ come from the terms $\bar{i}_{\rm NL1} \equiv 3\eta\xi_{\rm lin}^2\dot{\xi}_{\rm lin}$ and $\bar{i}_{\rm NL2} \equiv \eta\dot{\xi}_{\rm NL}$, where $\xi_{\rm NL}$ is the in-band motion due to nonlinear forces in (1). A lowest order estimate for $\xi_{\rm NL}$ is found by inserting the linear solution $\xi_{\rm lin}$ to the third-order force terms into (1) and using the linear response to find the corresponding motion at ω_3. One finds

$$\bar{i}_{\rm NL1} = -\frac{3}{4}\eta\omega_3\bar{u}_0^3 q^3\cos\omega_3 t \qquad (4a)$$

$$\bar{i}_{\rm NL2} = -\eta\omega_3\bar{u}_0^3 q\left[\frac{3}{4}q^2\cos\omega_3 t + \left(3q^3 + \frac{q}{4}\right)\sin\omega_3 t\right]. \qquad (4b)$$

Equating the amplitude of $\bar{i}_{\rm NL} = \bar{i}_{\rm NL1} + \bar{i}_{\rm NL2}$ with the amplitude of the fundamental current (3) at ω_1 and solving for the IIP3 voltage, we obtain

$$\bar{u}_{0,\rm IIP3}^2 = \frac{\omega_1}{\omega_3\sqrt{\left(3q^3 + \frac{q}{4}\right)^2 + \frac{9q^4}{4}}} \qquad (5)$$

where, as defined above, $q = k_e Q/\bar{k} = QC_0V^2/(k_b d^2 - 2C_0V^2)$. As ω_1 and ω_3 are almost equal, they can be canceled out. For high Q, $q > 1$ in (5) and the strongest nonlinear contribution is due to the ξ^3 term in (1). Thus, a simple estimate for the IIP3 voltage is obtained as

$$u_{0,\rm IIP3} = V\bar{u}_{0,\rm IIP3} \approx \frac{V}{\sqrt{3q^3}} \approx V\left(\frac{U_{\rm pi}}{V}\right)^3\sqrt{\frac{8}{3Q^3}} \qquad (6)$$

where $U_{\rm pi} = \sqrt{k_b d^2/(2C_0)}$ is the electromechanical pull-in voltage at which bias level the spring constant $\bar{k}$ vanishes and the resonator becomes unstable.

III. Single-Beam MEMS Resonator Example

To validate the analytical results, an experimental test with a clamped–clamped beam resonator was performed. The schematic of the resonator, fabricated on a silicon-on-insulator (SOI) wafer [3], is shown in Fig. 2(a) together with an illustration of the measurement setup. Harmonic signals at ω_1 and ω_2 within the filter bandwidth are generated with two Agilent 33120A signal sources. The filter output signal is amplified with a JFET preamplifier. The filter circuitry and the preamplifier are kept at a low pressure of 8×10^{-3} mbar. The output spectrum is measured with an HP 4195A network/spectrum analyzer. To model the resonator, the S_{21} measurement was performed for

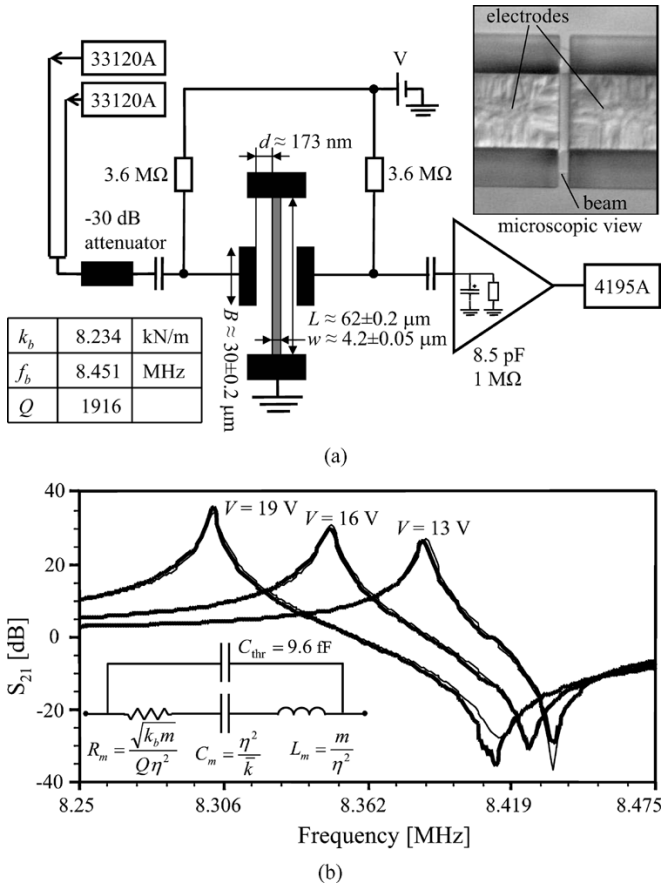

Fig. 2. Experimental setup for IIP3 measurement. (a) Measurement setup for the capacitively coupled beam resonator. The device thickness is 10 μm, and it vibrates horizontally in the plane of the wafer. Also shown are the relevant resonator parameters. Values for L, w, and B are estimated from the microscopic view while the gap size $d = 173$ nm and effective length $L_{\rm eff} = 66\ \mu$m ($> L$ due to imperfect clamping) are based on the numerical fit of Fig. 2(b). (b) Measured (thick line) and simulated (thin line) zero-bias-calibrated response of the beam resonator for different bias voltages. The electrical equivalent circuit is also shown ($R_m = 55$ kΩ, $C_m = 179.7$ aF, and $L_m = 2.022$ H at $V = 16$ V).

three different bias voltages well below the pull-in voltage, as shown in Fig. 2(b). Fitting an electromechanical model to the measured response allows one to find a good estimate of the filter parameters. Fitting was done by adjusting the effective beam length $L_{\rm eff}$, the Q value, the feed-through capacitance $C_{\rm thr}$, and the gap d. The obtained Q value is rather low due to the low aspect ratio L/w of the beam, resulting in energy leakage to supporting structures [7], [8]. The spring constant k_b is calculated from

$$k_b = \frac{16EH\left(\frac{w}{L}\right)^3}{\frac{1}{2}\left(\frac{B}{L}\right)^3 - \left(\frac{B}{L}\right)^2 + 1} \qquad (7)$$

which assumes the load to be uniformly distributed across the transducer area [9]. The eigenfrequency of the resonator is given by $f_b = 1.028\,w/L^2\sqrt{E/\rho}$ [10].

With the estimated parameter values, (6) gives 34.3 dBmV for IIP3 at $V = 16$ V (corresponding to -15.7 dBm with a 50-Ω source). This is compared to the measured behavior as well as to a two-tone harmonic-balance simulation [11] in Fig. 3. It is seen that all three approaches agree very well.

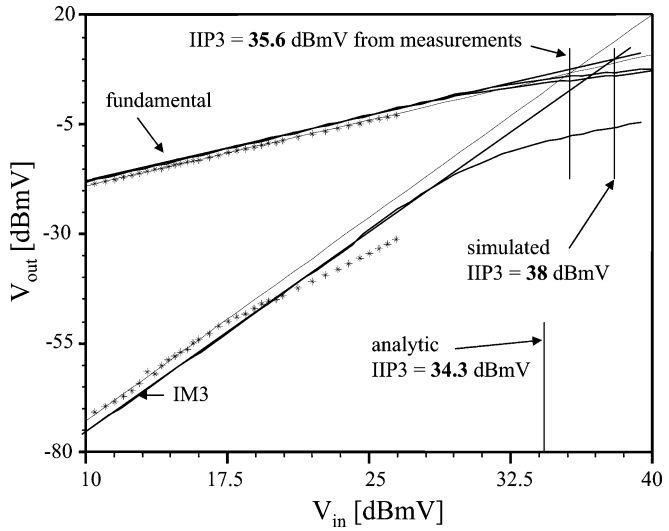

Fig. 3. Measured (asterisks) and simulated (solid curves) fundamental and IM3 voltage at the resonator output at $V = 16$ V and $\omega_2 - \omega_1 = 2\pi \times 200$ Hz (ω_1 and ω_2 are inside the filter passband). The lines extrapolate the linear behavior, found at small input voltages, to determine the IIP3.

IV. Discussion

In this letter, a concise formulation for IIP3 in capacitively coupled micromechanical filters is given. The experimental verification is given for a flexural clamped–clamped beam, but the formulation applies to all MEMS filters: 1) that are coupled with parallel-plate transducers and 2) for which the capacitive nonlinearities are the dominant intermodulation mechanism. Typically, for small gaps ($d < 200$ nm), the mechanical nonlinearities do not need to be taken into account [5].

As an example of usage of (6), the published values of $Q = 1600$, $d = 74$ nm $V = 12.9$ V, $k = 73.5$ MN/m, and $C_0 = 7.5$ fF for a demonstrated 1.1-GHz radial-mode disk resonator [4] give $u_{0,\mathrm{IIP3}} = 21$ kV while $R_m = 3.9\,\mathrm{M}\Omega$. It is thus seen that the motional impedance, rather than IM, is a challenge in using this resonator. The motional impedance can be lowered by increasing the bias voltage and reducing the electrode gap. However, while $R_m \propto d^4$, the IIP3 voltage is reduced even faster as $u_{0,\mathrm{IIP3}} \propto d^{9/2}$. For example, $d = 5$ nm and $V = 15$ V for the same resonator give $C_0 = 111$ fF, $u_{0,\mathrm{IIP3}} = 85$ mV, and $R_m = 60\,\Omega$. If this resonator were used as a bandpass filter, signal corruption due to IM can be expressed by a resulting signal-to-interference ratio $\mathrm{SIR} = u_{\mathrm{sig,in}}\, u_{0,\mathrm{IIP3}}^2 / u_{\mathrm{int,in}}^3$, where $u_{\mathrm{sig,in}}$ and $u_{\mathrm{int,in}}$ are the input signal and interference, respectively [12]. Using a GSM phone as an example, the specifications require operation with $u_{\mathrm{sig,in}} = -99$ dBm and $u_{\mathrm{int,in}} = -43$ dBm for the closest interferer [13]. With a 50-Ω antenna source, we find $\mathrm{SIR} = 7.3$ dB. This can be compared to the required receiver SIR of 9 dB [13]. Thus, it is concluded that IM specifications can set a lower limit for the gap in parallel-plate transducer coupled resonators.

Acknowledgment

The authors would like to thank J. Kiihamäki for device fabrication.

References

[1] T. Lee, *The Design of CMOS Radio-Frequency Integrated Circuits*, 2nd ed. Cambridge, U.K.: Cambridge Univ. Press, 2004.

[2] C. T.-C. Nguyen, "Frequency-selective MEMS for miniaturized low-power communication devices," *IEEE Trans. Microw. Theory Tech.*, vol. 47, no. 8, pp. 1486–1503, Aug. 1999.

[3] V. Kaajakari, T. Mattila, A. Oja, J. Kiihamäki, and H. Seppä, "Square-extensional mode single-crystal silicon micromechanical resonator for low phase noise oscillator applications," *IEEE Electron Device Lett.*, vol. 25, no. 4, pp. 173–175, Apr. 2004.

[4] J. Wang, Z. Ren, and C. T.-C. Nguyen, "Self-aligned 1.14-GHz vibrating radial-mode disk resonators," in *Proc. Transducers'03*, Jun. 2003, pp. 947–950.

[5] V. Kaajakari, T. Mattila, A. Oja, and H. Seppä, "Nonlinear limits for single-crystal silicon microresonators," *J. Microelectromech. Syst.*, vol. 13, no. 5, pp. 715–724, Oct. 2004.

[6] R. Navid, J. R. Clark, M. Demirci, and C. T.-C. Nguyen, "Third-order intermodulation distortion in capacitively-driven cc-beam micromechanical resonators," in *Proc. Int. IEEE Micro Electro Mechanical Systems Conf.*, Interlaken, Switzerland, Jan. 2001, pp. 228–231.

[7] T. Mattila, O. Jaakkola, J. Kiihamäki, J. Karttunen, T. Lamminmäki, P. Rantakari, A. Oja, H. Seppä, H. Kattelus, and I. Tittonen, "14 MHz micromechanical oscillator," *Sens. Actuators A, Phys.*, vol. 97–98, pp. 497–502, Apr. 2002.

[8] K. Y. Yasumura, T. D. Stowe, E. M. Chow, T. Pfafman, T. W. Kenny, B. C. Stipe, and D. Rugar, "Quality factors in micron- and submicron-thick cantilevers," *J. Microelectromech. Syst.*, vol. 9, no. 1, pp. 117–125, Mar. 2000.

[9] Q. Meng, M. Mehregany, and R. L. Mullen, "Theoretical modeling of microfabricated beams with elastically restrained supports," *J. Microelectromech. Syst.*, vol. 2, no. 3, pp. 128–137, Sep. 1993.

[10] W. Weaver Jr., S. P. Timoshenko, and D. H. Young, *Vibration Problems in Engineering*, 5th ed. New York: Wiley, 1990.

[11] T. Veijola and T. Mattila, "Modeling of nonlinear micromechanical resonators and their simulation with the harmonic-balance method," *Int. J. RF Microw. Computer-Aided Eng.*, vol. 11, no. 5, pp. 310–321, Sep. 2001.

[12] B. Razavi, *RF Microelectronics*. Upper Saddle River, NJ: Prentice-Hall, 1998.

[13] ETSI, *GSM Global System for Mobile Communications*, 3GPP TS 05.01/05.05, 2003.